A laboratory on the four-point probe technique

Andrew P. Schuetze
Edgewood Academy, San Antonio, Texas 78237

Wayne Lewis, Chris Brown, and Wilhelmus J. Geerts[a)]
Department of Physics, Texas State University at San Marcos, San Marcos, Texas 78666

(Received 6 September 2002; accepted 30 September 2003)

We describe how a classic electrostatics experiment can be modified to be a four-point probe lab experiment. Students use the four-point probe technique to investigate how the measured resistance varies as a function of the position of the electrodes with respect to the edge of the sample. By using elementary electromagnetism concepts such as the superposition principle, the continuity equation, the relation between electric field and electric potential, and Ohm's law, a simple model is derived to describe the four-point probe technique. Although the lab introduces the students to the ideas behind the Laplace equation and the methods of images, advanced mathematics is avoided so that the experiment can be done in trigonometry and algebra based physics courses. In addition, the experiment introduces the students to a standard measurement technique that is widely used in industry and thus provides them with useful hands-on experience.
[DOI: 10.1119/1.1629085]

I. INTRODUCTION

We describe how a classic laboratory experiment on electrostatics can be applied with some minor modifications to study the four-point probe measurement technique. The four-point probe technique is one of the most common methods for measuring resistivity.[1] The classic arrangement is to have four needle-like electrodes in a linear arrangement with a current injected into the material via the outer two electrodes. The resultant electric potential distribution is measured via the two inner electrodes [see Fig. 1(a)]. By using separate electrodes for the current injection and for the determination of the electric potential, the contact resistance between the metal electrodes and the material will not show up in the measured results.[2,3] Because the contact resistance can be large and can strongly depend on the condition and materials of the electrodes,[4] it is easier to interpret the data measured by the four-point probe technique than results gathered by two-point probe techniques.

The four-point probe technique was originally developed by Wenner in 1916 to measure the earth's resistivity.[5] In geophysics it is referred to as Wenner's method. In 1954 Valdes adopted the technique for semiconductor wafer resistivity measurements. The technique has also been applied to characterize electrolytes[6] and to analyze gases.[7]

Today the four-point probe technique is widely used in the semiconductor industry to monitor the production process. Electrical measurements are done on test structures to provide information on the various process steps. For example, resistivity measurements on doped semiconductor structures provide information on the active charge carrier concentration and the mobility and is used as feedback to the doping process. Resistivity measurements on aluminum test structures provide information on the linewidth and thickness of the interconnect, which is used to fine-tune the lithography process. In order to save space on the wafer, these test structures are integrated in the saw paths between the integrated circuits. Figure 2 shows a poly van der Pauw structure. It is used during the production process to monitor the properties of the poly-silicon, one of the many materials used to make integrated circuits. The square in the middle of the picture is the actual test-structures. At the top and bottom of the picture, two bonding pads, through which the electrical connections are made, are visible. As the price of silicon is comparable to the price of real estate in the center of Tokyo, chip manufacturers try to limit the space on a wafer that is used by test structures. From this point of view it is important to understand how the size of the test structures and the position of the electrodes or contacts influence the measured current, I, and the measured electric potential, V.

In general, the material's sheet resistivity, ρ, can be calculated by the relation[1,2] $\rho = \mathrm{RCF}(V_{\mathrm{measured}}/I_{\mathrm{measured}})$. The resistivity correction factor (RCF) takes the size of the test structure, the thickness of the material, the size of the electrodes, and the position of the electrodes with respect to the boundary of the test structure into account. Figure 1(b) illustrates the effect of the position of the electrodes with respect to the boundaries of the test structure. By placing the electrodes at the edge rather than in the middle of the test structure, the measured voltage over the inner electrodes will be two times larger because all current has to take the right-half plane. Valdes calculated the RCF for probes parallel and perpendicular to the boundary of a slab.[2] Others have modified the linear arrangement of the electrodes and included different geometrical patterns.[8–10]

Figure 2 shows a square configuration[8,9] that is widely used in the semiconductor industry. Calculations on more exotic configurations can be found in Ref. 10. Although most of those papers contain advanced mathematics, we will show below that the effect of boundaries on the results obtained with a four-point probe can be understood using standard concepts from electromagnetism and algebraic manipulations. Furthermore, we will show that these boundary effects can be demonstrated using a setup from a classic electrostatics lab experiment.

II. APPARATUS

Our four-point probe setup is sketched in Fig. 3. It uses the equipment of a common college physics experiment on equi-

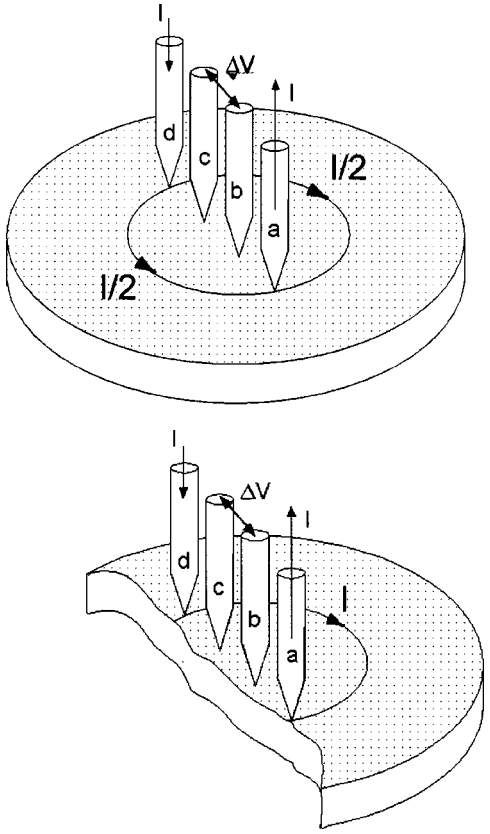

Fig. 1. (a) Four-point probe measurement technique. (b) Probe near the edge of the sample; all current has to go through the left half plane.

potential surfaces and field lines. The two-dimensional medium is a clear plastic tray filled with water. The depth of the water models the thickness of the material to be investigated and will be referred to as the film thickness of the medium. Working in an aqueous system has several advantages. First of all, it is an easily obtainable source of material. There is also no possibility of damaging the surface by scratching or other deformations. Nothing more than a caliper set is required to measure the thickness of the material under study, that is, the depth of the water. Varying the thickness also is simple. We can easily add more water to the tray as well as submerge the glass plates to create regions of varying resistance. Finally, it is simple to automate the measurements by dragging the probe through the water and using a computer interface to collect and plot the resistivity data as a function of the position of the electrodes with respect to the edge of the water tray. In the rest of the paper we will refer to such an automatic measurement as a scan.

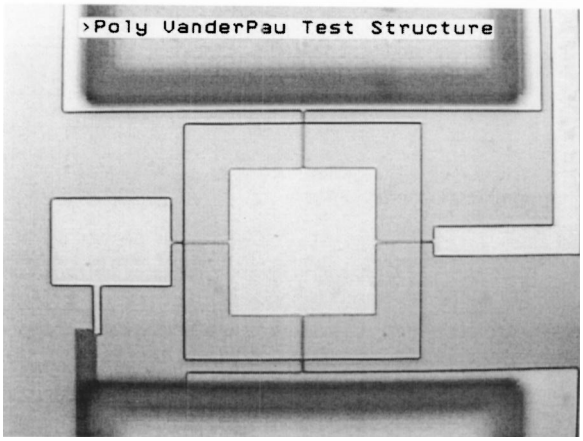

Fig. 2. Process monitors in the saw-path between the integrated circuits on a wafer (courtesy of Dr. Daniel Chesire of Lucent Technology).

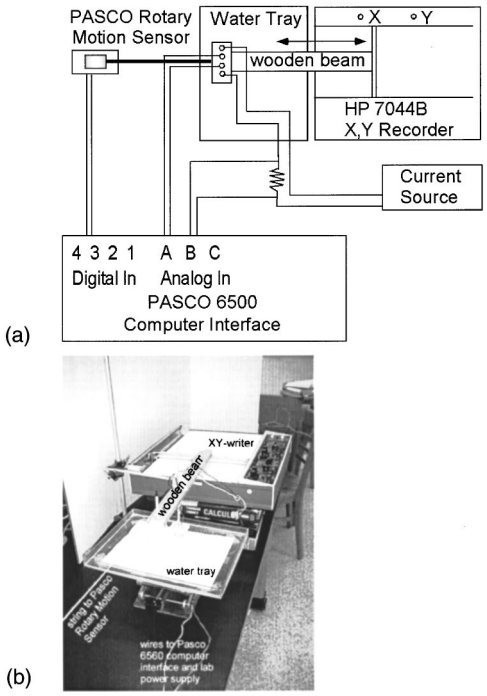

Fig. 3. Four-point probe measurement system: (a) schematic drawing; (b) picture of setup.

The four-point probe was constructed out of Singer sewing machine needles that were inserted into predrilled holes in a small block of polyethylene plastic. The latter was obtained by cutting a small piece from a kitchen cutting board. The electrode holes were carefully drilled to be 1 cm apart. The probe was attached to a 30-in. wooden beam by means of a wooden dowel. It was not permanently glued to the beam so that it could be rotated 90° for the parallel and perpendicular scans. All of the connecting wire pairs were twisted and all of the connections were soldered. The wooden beam was connected to the penholder of an X/Y writer. By using the time base of the X/Y writer, the four-point probe could be dragged through the water. The position of the probe could be determined from a Pasco rotary motion sensor. A string connected to the wooden beam moving tangentially over the small pulley of the sensor coupled the probe and motion sensor (see Fig. 3). A simple lab power supply provided a constant current of 4–8 mA. Current, voltage, and position were read into a computer via a Pasco 6560 computer interface. The Pasco software provided an easy platform to plot resistance as a function of position in real time. A typical resistance scan took between 1 and 2 min. All scans were done in tap water. Better results in terms of reproducibility are to be expected by using a better-defined electrolyte than hard water from the tap. Preliminary experiments with a 0.01-M HCl solution look very promising.

III. EXPERIMENTAL RESULTS

Figure 4 shows a typical plot of the reciprocal resistance $(1/R = I_{\text{measured}}/V_{\text{measured}} = \text{RCF}/\rho)$ as a function of the dis-

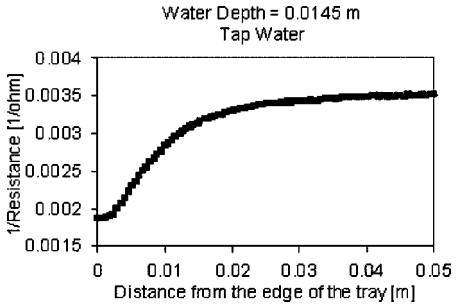

Fig. 4. Reciprocal resistance as a function of the distance to the edge of the tray.

tance to the edge of the tray. The line of electrodes was kept parallel to the boundary as shown in Fig. 1(b). Close to the edge of the tray, the reciprocal resistance is approximately two times smaller than in the middle of the tray. Because the resistivity, ρ, is a constant, the RCF close to the edge of the tray is approximately two times smaller than that in the middle of the water tray. If we place the probe at the edge of the sample all the current is forced to go through the right half plane. In the case where the probe is placed in the middle of the sample, the current has two paths, i.e., the right and left half plane, with each having equal resistance (see also Fig. 1). The measured reciprocal resistance and RCF will thus be a factor 2 larger in the middle of the sample. Approximately 4 cm away from the boundary (four times the electrode distance), the RCF becomes independent of the position. At 0.5 cm away from the edge, a bending point appears to exist. The data in Fig. 4 clearly show that we have to stay approximately four times the electrode distance away from the edge of the sample to obtain position independent values of the resistance and avoid having to use the RCF.

Figure 5 shows a series of scans over submerged glass plates of different thicknesses. The depth in the deeper part of the tray was 2.5 cm for all the scans. In the shallow area of the tray the resistance is larger than in the deeper waters. The glass plates were approximately 7.5 cm long. In all the scans there is a transition area of approximately 3 cm between the high resistance and low resistance area. This experiment clearly illustrates that the measured values do not reflect the local values of the resistance, but rather the average value originating from an area of approximately three times the electrode distance. So although the four-point probe technique can be used in inhomogeneous samples, for example,

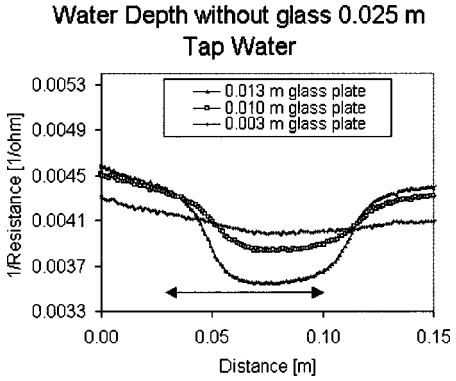

Fig. 5. Resistance scan over submerged glass plates.

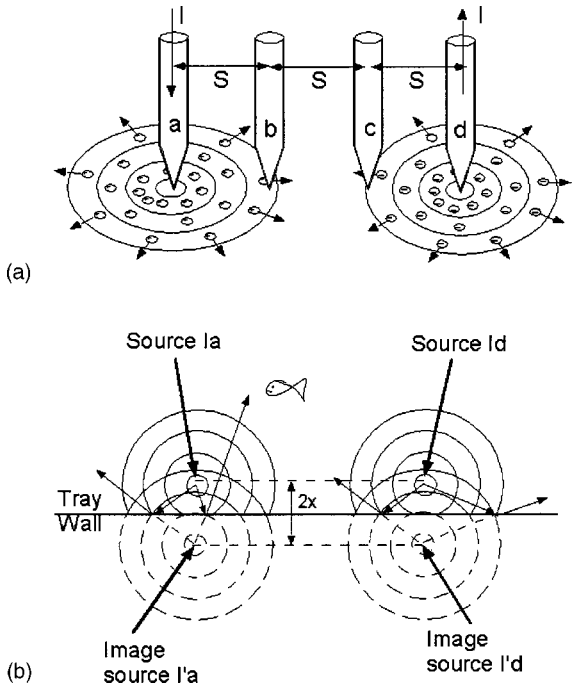

Fig. 6. (a) Charged particle flux for an infinite large tray; (b) reflection of the charged particle of the edges of the tray. Top view; the directions of four different charged particles are indicated. In (a) and (b) the circles indicate iso-current density surfaces of the contribution of that particular source.

samples whose thickness or resistivity is not a simple constant, the distance between the electrodes limits the lateral resolution of the measurement technique.

The slope in the graphs of Fig. 5 for small values of the distance is a measurement artifact. The wooden beam used in the experiment appeared to be slightly curved, which caused the electrode depth to be slightly dependent on the position of the probe. This effect resulted in a background signal that shows up as a residual slope for positions close to the edge of the tray.

IV. THEORY

The electric potential around the electrodes can be calculated by solving Laplace's equation, which is a combination of the equation of continuity ($I_{\text{in}}=I_{\text{out}}$), Ohm's law ($V=IR$), and the $E-V$ relation ($E=-dV/dx$):

$$\nabla \vec{J}=\nabla \frac{\vec{E}}{\rho}=\frac{\nabla^2 V}{\rho}=0. \tag{1}$$

It can be shown that a solution of Eq. (1) that satisfies the given boundary conditions is unique.[11] This uniqueness theorem often is used in combination with the method of images to find the solution for V in an intuitive way. Laplace's equation, however, can be quite intimidating and is beyond the level of an introductory physics course. We believe, however, that the technique of image sources can be understood in a conceptual way without introducing Eq. (1), because we are concerned with current sources that can be visualized as sources that inject charged particles into the conducting layer.

In Fig. 6(a) the two current injection electrodes are depicted in the middle of an infinite water tray. Each sprays charged particles in all directions into the water. Close to the

electrodes the current density (**J**) will be large, while further away **J** will decrease because the same charge will be distributed over a half sphere with a larger surface. The total current density at a particular point is the sum of the current density from the positive electrode and the current density from the negative electrode. To understand what happens when the electrodes approach a boundary, we assume that when a charged particle collides with the walls of the plastic water tray, it will bounce back just like a ping-pong ball bounces off a table. Those reflected charged particles can be considered to originate from a virtual electrode, the image source, at the other side of the tray wall [see Fig. 6(b)]. So instead of taking all possible reflections into account, we introduce an image source on the other side of the boundary. The total current density at a particular point close to the wall is the sum of the current densities originating from both electrodes and the current densities of their image sources (the reflected particles). The components of **J** perpendicular to the interface cancel each other out and the current density will have only a component parallel to the edge of the water tray. From the current density distribution the electric field distribution, **E**, can be calculated using Ohm's law. **E** can be used to calculate the electric potential (the slope of the electric potential is the electric field). This calculation can be quite cumbersome because **J** and **E** are vector quantities, and the latter step involves integration techniques.

A short cut can be provided for non-calculus-based physics courses by using the superposition rule for the electric potential, the relation between the electric field and the electric potential of a point source, and some straightforward algebra. We know that the electric field and electric potential around an electric point charge are given by

$$|\vec{E}|=\frac{kQ}{r^2}, \tag{2a}$$

$$V=\frac{kQ}{r}, \tag{2b}$$

with $V=|\vec{E}|r$ and $k=9\times10^9\ \mathrm{Nm^2/C^2}$. The current injected in the material will result in a similar distribution of the electric field. If we assume that the injected current I will be distributed over a half sphere of radius r, the electric field will be given by

$$|\vec{E}|=|\vec{J}|\rho=\frac{I}{\frac{1}{2}4\pi r^2}\rho=\frac{I\rho}{2\pi r^2}. \tag{3}$$

Because the electric field of Eqs. (2a) and (3) has the same form, we can use Eq. (2b) to calculate the electric potential in the material. We then combine Eqs. (2) and (3) to obtain the electric potential around a point source that injects a current I in the water:

$$V=\frac{I\rho}{2\pi r}. \tag{4}$$

Equation (4) can be used to calculate the electric potential at the position of the sensing probes b and c, that is, V_b and V_c. For the electric potential of each sensing probe we have four contributions: two originating from the real current injection electrodes, I_a and I_d, and two from their virtual image sources, I_a' and I_d':

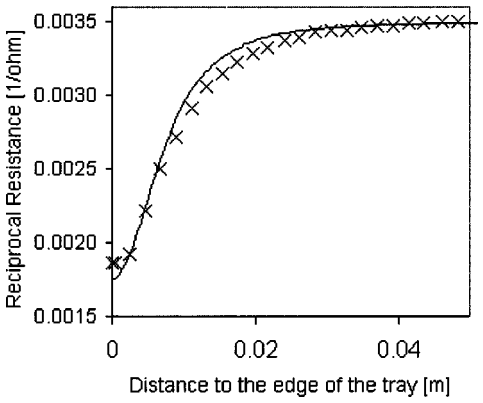

Fig. 7. Calculated reciprocal resistance as a function of the distance to the edge of the tray.

$$V_b=V_b(I_a)+V_b(I_d)+V_b(I_a')+V_b(I_d')$$
$$=\frac{I\rho}{2\pi}\left[-\frac{1}{s}+\frac{1}{2s}-\frac{1}{\sqrt{s^2+(2x)^2}}+\frac{1}{\sqrt{(2s)^2+(2x)^2}}\right], \tag{5}$$

$$V_c=V_c(I_a)+V_c(I_d)+V_c(I_a')+V_c(I_d')$$
$$=\frac{I\rho}{2\pi}\left[-\frac{1}{2s}+\frac{1}{s}-\frac{1}{\sqrt{(2s)^2+(2x)^2}}+\frac{1}{\sqrt{s^2+(2x)^2}}\right], \tag{6}$$

$$\frac{\mathrm{RCF}}{\rho}=\frac{I_{\mathrm{measured}}}{V_{\mathrm{measured}}}$$
$$=\frac{1}{V_c-V_b}$$
$$=\frac{2\pi}{\rho}\left[\frac{1}{\frac{1}{s}-\frac{2}{\sqrt{(2s)^2+(2x)^2}}+\frac{2}{\sqrt{s^2+(2x)^2}}}\right], \tag{7}$$

where s is the electrode distance, and x is the distance to the edge of the tray.

We used a spreadsheet program to make a plot of Eq. (7) (the solid line in Fig. 7). We also plotted some of the measured data (indicated by the symbol $\times$) in Fig. 7. Good agreement is obtained between theory and experiment. Even the bending point at 0.5 s shows up in the measurement results. The small discrepancies between the calculated and measured data can be understood by realizing that our calculation is only an approximation. Our water tray has a finite depth, which means that the charged particles will also bounce off the bottom of the tray. So we should also consider mirror sources below and above the water tray. Each reflection requires the introduction of a new virtual source. Because the number of reflections for a layer with finite thickness is infinite, the number of virtual sources also will be infinite. The contribution of the sources far away from the water will, however, be negligible, which means that we only have to add the contributions of the closest sources to obtain a reasonable approximation. Further differences between the measured and calculated data are due to imperfections of our experimental setup, that is, contamination of the electrodes caused by electrochemical effects during the experiments and a slight bending of the wooden beam.

V. SUMMARY

We have adapted a classic experiment on electrostatics to an experiment on the four-point probe measurement technique. The new experiment introduces students to the same concepts at the original one, that is, the superposition principle, the continuity equation, the relation between electric field and electric potential, and Ohm's law. In addition, it gives a clear example of how the laws of electromagnetism can be applied in a practical situation. Although we used a water tray for the conducting medium, conducting paper or rubber, which are used at many institutions, would be equally suitable. In that case gold plated spring driven contacts should be used.

ACKNOWLEDGMENTS

The authors are happy to acknowledge Dr. Joe Koke and Dr. Linette Watkins for providing the glass work and *p*H indicator that were instrumental in finding the right electrolyte. We also would like to thank Kenneth Nemson of Pasco Inc. for providing the rotary motion sensor and Dr. William Jackson of SWT for proofreading the manuscript. This work was funded by Southwest Texas State University's Science/Math/Technology Education Institute, the Research Corporation, the division of materials research of NSF under Grant No. 0075372, and an indirect cost fellowship grant of the School of Science of SWT.

[a]Electronic mail: wjgeerts@txstate.edu

[1]Dieter K. Schroder, *Semiconductor Material and Device Characterization* (Wiley, New York, 1990).
[2]L. B. Valdes, "Resistivity measurements on germanium for transistors," Proc. IRE **42**, 420–427 (1954).
[3]Brian Jones, "Resistance measurements on play-doh TM," Phys. Teach. **31**, 48–49 (1993).
[4]Rolf E. Hummel, *Electronic Properties of Materials* (Springer, New York, 1993).
[5]F. Wenner, "A method of measuring earth resistivity," Bur. Stand. (U.S.) Bull. **12**, 469–478 (1915).
[6]S. P. S. Badwal, F. T. Ciacchi, and D. V. Ho, "A fully automated four-probe D.C. conductivity technique for investigating solid electrolytes," J. Appl. Electrochem. **21**, 721–728 (1991).
[7]Norio Miura, T. Harada, and N. Yamazoe, "Sensing characteristics and working mechanism of four-probe type solid-state hydrogen sensor using proton conductor," J. Electrochem. Soc. **136**, 1215–1219 (1989).
[8]Arthur Uhlir, Jr., "The potentials of infinite systems of sources and numerical solutions of problems in semiconductor engineering," Bell Syst. Tech. J. **34**, 105–128 (1955).
[9]L. J. van der Pauw, "A method of measuring specific resistivity and Hall effect of discs of arbitrary shape," Philips Res. Rep. **13**, 1–9 (1958).
[10]Masato Yamashita, "Resistivity correction factor for the four-circular-probe method," Jpn. J. Appl. Phys., Part 1 **32**, 246–251 (1993).
[11]David K. Cheng, *Field and Wave Electromagnetics* (Addison–Wesley, Reading, MA, 1989).